

Constraining Ω with Cluster Evolution

Neta A. Bahcall, Xiaohui Fan, and Renyue Cen
Princeton University Observatory
Peyton Hall
Princeton, NJ 08544-1001
electronic mail : neta,fan,cen@astro.princeton.edu

Abstract

We show that the evolution of the number density of rich clusters of galaxies breaks the degeneracy between Ω (the mass density ratio of the universe) and σ_8 (the normalization of the power spectrum), $\sigma_8 \Omega^{0.5} \simeq 0.5$, that follows from the observed present-day abundance of rich clusters. The evolution of high-mass (Coma-like) clusters is strong in $\Omega = 1$, low- σ_8 models (such as the standard biased CDM model with $\sigma_8 \simeq 0.5$), where the number density of clusters decreases by a factor of $\sim 10^3$ from $z = 0$ to $z \simeq 0.5$; the same clusters show only mild evolution in low- Ω , high- σ_8 models, where the decrease is a factor of ~ 10 . This diagnostic provides a most powerful constraint on Ω . Using observations of clusters to $z \simeq 0.5 - 1$, we find only mild evolution in the observed cluster abundance. We find $\Omega = 0.3 \pm 0.1$ and $\sigma_8 = 0.85 \pm 0.15$ (for $\Lambda = 0$ models; for $\Omega + \Lambda = 1$ models, $\Omega = 0.34 \pm 0.13$). These results imply, if confirmed by future surveys, that we live in a low-density, low-bias universe.

subject headings : galaxies : clusters – galaxies : evolution – galaxies : formation – cosmology : theory – cosmology : observation – dark matter

1. Introduction

The observed present-day abundance of rich clusters of galaxies places one of the strongest constraints on cosmology (Bahcall and Cen 1992, White *et al.* 1993, Eke *et al.* 1996, Viana and Liddle 1996, Pen 1996): $\sigma_8 \Omega^{0.5} \simeq 0.5 \pm 0.05$, where σ_8 is the normalization of the power spectrum on $8 \text{ h}^{-1} \text{ Mpc}$ scale (reflecting the *rms* mass fluctuations on this scale), and Ω is the present value of the cosmological density parameter. This constraint is degenerate in $\Omega - \sigma_8$; models with $\Omega = 1$ and $\sigma_8 \simeq 0.5$ are indistinguishable from models with $\Omega \simeq 0.25$ and $\sigma_8 \simeq 1$. (A $\sigma_8 \simeq 1$ universe implies no bias in the distribution of mass versus light, since $\sigma_8(\text{gal}) \simeq 1$ is observed for galaxies; a $\sigma_8 \simeq 0.5$ universe, on the other hand, is highly biased, with mass distributed more widely than light).

In the present paper, we show that a study of the evolution of the number density of

rich, massive clusters as a function of redshift will break the degeneracy between Ω and σ_8 and determine each parameter independently. The growth of high mass clusters depends strongly on the cosmology — mainly Ω and σ_8 (e.g., Press and Schechter 1974, Peebles 1993, Cen and Ostriker 1994a, Jing and Fang 1994, Eke *et al.* 1996, Viana and Liddle 1996). In low-density models, density fluctuations evolve and freeze out at early times, thus producing only little evolution at recent times ($z \lesssim 1$). In an $\Omega = 1$ universe, the fluctuations start growing only recently thereby producing strong evolution in recent times: a large increase in the number density of massive clusters is expected from $z \sim 1$ to $z = 0$. The evolution is so strong that finding even $\sim 1 - 2$ Coma-like mass clusters at $z \simeq 0.5$ over $\sim 10^3 \text{ deg}^2$ of sky would rule out an $\Omega = 1, \sigma_8 \simeq 0.5$ model, where only $\sim 10^{-2}$ such clusters would be expected (§3).

We investigate in this paper the evolution of the mass function (MF) of clusters (the number density of clusters above a given mass) for various cosmologies using large-scale N-body simulations, and compare the results with cluster observations to $z \simeq 0.5 - 1$.

2. Model Simulations

We investigate the evolution of the cluster MF in five cosmological models using large-scale numerical simulations. The models include: Standard Cold Dark Matter (SCDM; $\Omega = 1$), normalized to a present-day mass fluctuation on $8h^{-1} \text{ Mpc}$ scale of $\sigma_8 = 1.05$ (consistent with the COBE microwave background fluctuations on large scales); a biased SCDM ($\Omega = 1$), with low normalization ($\sigma_8 = 0.53$), which fits the present day cluster abundance (but is inconsistent with the COBE normalization); a low-density, Λ dominated CDM model (LCDM), and an open CDM model (OCDM); and a mixed, hot and cold dark matter model (MDM, $\Omega=1, \Omega_p=0.3$; from Cen and Ostriker 1994b, normalized to $\sigma_8=0.6$, consistent with the present day cluster abundance). Table 1 summarizes the model parameters. All models, except for the COBE-normalized SCDM ($\sigma_8 \simeq 1$), are consistent with the present day cluster abundance (Bahcall and Cen 1992, White *et al.* 1993, Cen and Ostriker 1994b, Eke *et al.* 1996, Pen 1996). The SCDM $\sigma_8 \simeq 1$ model over-produces the number of massive clusters by an order of magnitude. All models except for the biased SCDM ($\sigma_8 \sim 0.5$) are also consistent with the COBE normalization (Bunn & White 1996).

A large-scale particle-mesh code with box size $400 h^{-1} \text{ Mpc}$ was used to simulate the evolution of the dark matter in the models. A large simulation box is needed in order to produce a significant number of the rich but rare clusters ($\lesssim 10^{-5} h^3 \text{ clusters Mpc}^{-3}$). The simulation box contains 720^3 cells and $240^3 = 10^{7.1}$ dark matter particles, with a particle mass of $1.3 \times 10^{12} \Omega h^{-1} M_\odot$. In each simulation, clusters are selected as the maxima of the

mass distribution within spheres of comoving radius of $1.5h^{-1}$ Mpc. The mass of each cluster is determined within two relevant radii: a co-moving radius of $R_{\text{com}} = 1.5h^{-1}$ Mpc, and a physical radius of $R_{\text{phy}} = 1.0h^{-1}$ Mpc. We use these radii in order to allow a proper comparison with observations, which generally employ R_{com} or R_{phy} as their observable parameter. A virial cluster radius, which is commonly used in theoretical analyses (such as the Press-Schechter approximation), generally cannot be accurately determined from observations. To study the evolution of the cluster mass function, cluster masses are determined at several redshifts: $z = 0, 0.5, 1$ and 2 . The cluster MF, $n(>M)$, which represents the number density of clusters above a given mass threshold is then determined at each redshift. The evolution of the cluster mass function is derived for each model and compared with observations.

3. Evolution of the Cluster Mass Function

The evolution of the cluster MF is presented in Fig. 1 for two representative models : biased $\Omega=1$ SCDM and low-density OCDM, which are “degenerate” at $z = 0$. A negative evolution of the cluster MF is seen in all models — i.e., the abundance of clusters decreases at earlier epochs for clusters of a given mass, since massive clusters grow with time (e.g., Press and Schechter 1974, Peebles *et al.* 1989, Peebles 1993, Cen and Ostriker 1994a, Luppino and Gioia 1995, Eke *et al.* 1996). The *rate* of the evolutionary growth, however, is strongly model dependent. For example, the number density of $M(\leq 1.5) \geq 3 \times 10^{14}h^{-1}M_{\odot}$ clusters drops by a factor of ~ 40 from $z = 0$ to $z = 0.5$ in the biased SCDM cosmology, while the drop is only a factor of 4 (instead of 40) in the low-density models (OCDM, LCDM). The difference becomes even larger for more massive clusters (see below).

The evolution of the cluster density as a function of redshift is presented in Fig. 2 for massive clusters with mass $M(\leq R_{\text{com}} = 1.5h^{-1}\text{Mpc}) \geq 5.5 \times 10^{14}h^{-1}M_{\odot}$ (corresponding to richness class $\gtrsim 2.5$; Bahcall and Cen 1993), and in Fig. 3 for less massive clusters $M(\leq R_{\text{phy}} = 1.0h^{-1}\text{Mpc}) \geq 1.5 \times 10^{14}h^{-1}M_{\odot}$ (corresponding to richness class $\gtrsim 0$, see also §4). At $z \simeq 0$, all models except $\sigma_8 \simeq 1$ SCDM yield a comparable abundance of clusters, consistent with observations. The $\sigma_8 \sim 1$ SCDM model produces an order-of-magnitude more clusters than observed. At high redshifts, the abundance of clusters decreases sharply for the low σ_8 models but the decrease is slow for higher σ_8 . The evolution rate is insensitive to the value of the Hubble constant, or the exact shape of the power spectrum, and is most sensitive to the normalization σ_8 (for same mass clusters). The dependence on Ω itself is in fact only secondary. The strong exponential dependence on σ_8 results from the fact that for a given *mass* cluster, a lower σ_8 implies the clusters are rarer peaks in the density distribution, therefore evolving considerably faster than in high σ_8 models (see Fan *et al.* 1997). An observational determination of the cluster evolution rate therefore enables us to directly constrain σ_8 .

4. Comparison with Observations

Systematic observations of clusters of galaxies at high redshifts are only now beginning, with the use of complete redshift surveys (determining cluster mass from velocity dispersion), X-ray observations (temperatures of clusters), and weak gravitational lensing. New complete surveys of optical and x-ray clusters at low to high redshifts ($z \gtrsim 0.5$) will become available over the next several years. Here we present results from two independent current optical cluster surveys in the redshift range $z \simeq 0$ to ~ 1 . While the current samples are still small and the uncertainties large, the sensitive cluster evolution already allows us to place strong constraints on the cosmology.

The CNOC optical cluster redshift survey (Carlberg *et al.* 1996) represents a small but complete redshift survey of high mass clusters in the redshift range $z = 0.18 - 0.55$, with an EMSS extension at $z = 0.55 - 0.85$ (Henry *et al.* 1992, Luppino and Gioia 1995, Carlberg *et al.* 1997). Redshifts for typically ~ 30 to > 100 galaxies per cluster are used to accurately determine the velocity dispersion and mass of each cluster (Carlberg *et al.* 1996). The cluster mass threshold and cluster densities in the survey, properly corrected for completeness effects, are discussed by Carlberg *et al.* (1997). The mass threshold used is based on a velocity dispersion threshold of $\sigma_r \geq 800 \text{ km s}^{-1}$, which corresponds to a mass (within $R_{\text{com}} = 1.5 h^{-1} \text{ Mpc}$) of $M(\leq 1.5) \geq 5.5 \times 10^{14} h^{-1} M_{\odot}$ (as determined from the CNOC data as well as compared with Coma). The cluster densities above this threshold are $3.5 \times 10^{-7} \text{ Mpc}^{-3}$ at $z = 0.18 - 0.35$, and $9.3 \times 10^{-8} \text{ Mpc}^{-3}$ at $z = 0.35 - 0.55$ (for $\Omega = 1$). The high redshift extension at $z = 0.55 - 0.85$ (Luppino and Gioia 1995, Carlberg *et al.* 1997) does not have complete velocity measurements but contains the richest and most luminous X-ray clusters (some with observed velocity dispersions $\sigma_r \gtrsim 1200 \text{ km}$). We conservatively assume that these clusters have the same mass threshold as the CNOC clusters (also selected from EMSS). The mass threshold is likely to be higher; if so, this will raise the best-fit σ_8 value. This uncertainty is included in our estimates. The observed abundance of nearby clusters ($z \simeq 0 - 0.1$) is taken from Bahcall and Cen (1993), Mazure *et al.* (1996, the ESO survey) and Henry and Arnaud (1992; based on X-ray cluster selection), all converted to the common mass threshold of $5.5 \times 10^{14} h^{-1} M_{\odot}$ (using the observed MF, Bahcall and Cen 1993). This common mass threshold is slightly lower than a Coma-type cluster ($\sim 6.5 \times 10^{14} h^{-1} M_{\odot}$; Hughes 1989, Bahcall & Cen 1993). The sensitivity of the results to the exact mass threshold is tested by varying the assumed threshold from 5 to $6.5 \times 10^{14} h^{-1} M_{\odot}$; the results (§5) include these uncertainties.

The results are presented in Fig. 2, together with the model expectations for this mass threshold clusters. (The model σ_r and mass thresholds are corrected for the resolution effect of the simulation by comparing with high resolution simulations; the effect is small: $\lesssim 5\%$).

Only a mild negative evolution is observed. This mild evolution is in excellent agreement with the low-density high-normalization models (OCDM, LCDM); it is inconsistent by a factor of 10 – 100 with the very strong evolution expected in the biased ($\sigma_8 \simeq 0.5$) SCDM and MDM models. The expected cluster density decreases by a factor of ~ 10 from $z = 0$ to $z = 0.5$ in the low-density models, while the decrease becomes enormous ($\sim 10^3$) for $\sigma_8 \simeq 0.5$ SCDM, and $\sim 10^2$ for MDM. The data show a decrease by a factor of ~ 10 to $z \simeq 0.5$. This comparison differentiates the $\Omega = 1$, $\sigma_8 \simeq 0.5$ models from the $\Omega \simeq 0.3-0.4$, $\sigma_8 \simeq 0.8$ models, which are indistinguishable at $z \simeq 0$. Only the low-density, higher normalization models are acceptable at high redshifts (see §5). The unbiased $\sigma_8 \simeq 1$ SCDM model, which also yields mild evolution (due to its high σ_8), is inconsistent with the observed cluster abundance at any redshift.

The second cluster sample we investigate is the Palomar Distant Cluster Survey (PDCS; Postman *et al.* 1996). The PDCS is a complete automated survey of distant clusters to $z \sim 1$ from deep imaging CCD data over 5 deg^2 . Clusters were selected from the imaging data using a matched-filter algorithm, which yields best-fit estimates of the cluster richness (\propto luminosity) and redshift. While the clusters do not have measured redshifts and velocity dispersions (i.e., masses), the estimated luminosities are determined in a consistent manner from $z \simeq 0.2$ to ~ 1 , enabling us to investigate the evolutionary trend of the cluster densities. Measurements of the cluster redshifts and velocity dispersions will eventually provide more accurate results. We select all clusters with luminosities $L_{cl} \geq 50L^*$ (selected in the I -band, with richness threshold $\Lambda_{cl} \geq 50$ where $L_{cl} = \Lambda_{cl}L^*$ within a physical radius of $1h^{-1} \text{ Mpc}$, the radius used by the PDCS selection). This corresponds to a conservative mass threshold of $M(R_{\text{phy}} = 1h^{-1}\text{Mpc}) \gtrsim 1.5 \times 10^{14}h^{-1}\text{Mpc}$ for an average cluster $M/L \sim 300h$ (Bahcall *et al.* 1995, Carlberg *et al.* 1996). (The evolution results are not sensitive to the exact mass threshold at these low mass values; see below).

Figure 3 presents the evolution of the PDCS cluster density to $z \simeq 1$. The most distant point, at $z \simeq 0.9$, includes an incompleteness correction using the PDCS calibrated selection function at that redshift, and is thus less accurate. (The error bar includes both statistical uncertainties and a conservatively estimated uncertainty due to the selection correction). Figure 3 compares the observed evolution with the model expectations for the same physical radius and mass threshold clusters. The data, again, show only a minimal evolution of the cluster density, in excellent agreement with the low-density, high- σ_8 models. The data are inconsistent with the biased SCDM and MDM models, which predict ~ 10 times lower cluster density than observed at $z \sim 1$. (If the actual mass threshold of the clusters is larger than estimated above, then the model evolution will be even stronger and the evolutionary difference among models somewhat larger; in that respect the assumed mass threshold is a conservative choice).

The results are similar for the PDCS and the CNOC samples. While the CNOC clusters represent considerably higher mass clusters, which are most sensitive to the cosmology, the PDCS clusters reach to higher redshifts of $z \sim 1$. The fact that both independent samples, with different mass threshold clusters and different selection algorithms, yield similar results provides further support to these conclusions.

5. Constraining Ω

A comparison of the observed cluster evolution with the models shows that the data are consistent with the low-density models (OCDM and LCDM), and are inconsistent with the $\Omega = 1$ models (SCDM, biased SCDM and MDM). The relatively mild evolution observed in both the CNOC and PDCS samples is consistent with OCDM at a significance level of $\sim 60\%$ (based on a χ^2 test), and with LCDM at $\sim 30\%$. The $\Omega = 1$ SCDM and MDM models are rejected at $> 99.9\%$.

We use the data to directly determine the best-fit values of Ω and σ_8 for the CDM models. We use the method described by Fan *et al.* (1997), correlating the evolution rate ($n(z)/n(0)$) with σ_8 to determine σ_8 directly, since the primary dependence of the evolution rate is on σ_8 (for same mass clusters). The evolution rate is exponentially dependent on σ_8^2 – increasing strongly as σ_8 decreases; it is nearly independent of other parameters, including Ω (see Fan *et al.*). We determine the best-fit relation for the evolution rate versus σ_8 from the model simulations and compare the expected relation with the observed evolution rate. We find $\sigma_8 = 0.85 \pm 0.15$. The observed mild evolution rate of rich clusters thus implies a nearly unbiased universe; a strongly biased universe ($\sigma_8 < 0.7$) is unlikely since it produces considerably stronger evolution than observed. The results are consistent with those of Carlberg *et al.* (1997) of $\sigma_8 = 0.75 \pm 0.1$. Combined with the $\Omega - \sigma_8$ relation for present-day cluster abundance for CDM models (from Eke *et al.* 1996), we find $\Omega = 0.3 \pm 0.1$ (for $\Lambda = 0$), and $\Omega = 0.34 \pm 0.13$ (for $\Lambda = 1 - \Omega$). The results are presented in Fig. 4. The figure illustrates the powerful diagnostic of cluster evolution in determining Ω and σ_8 ; it places the strongest constraints yet on these parameters. The independent constraint placed by cluster dynamics, $\Omega \simeq (0.2 \pm 0.07)\sigma_8^{-1}$ (assuming linear bias; Bahcall *et al.* 1995, Carlberg *et al.* 1996, 1997) is also shown in the figure; it is consistent with the above results, yielding $\Omega = 0.24 \pm 0.1$ for $\sigma_8 = 0.85 \pm 0.15$. This Ω range provides the overlap of the constraints placed by the cluster abundance evolution and cluster dynamics observations. These results suggest that we live in a low-density, low-bias universe. Recent observations suggesting a minimal negative evolution of the X-ray cluster luminosity function (Henry *et al.* 1992, Castander *et al.*, 1994, Collins *et al.* 1997, Nichol *et al.* 1997, Mushotzsky *et al.* 1997) are

also consistent with the above findings.

We thank J.P.Ostriker, J.P.E.Peebles, D.N.Spergel and M.A.Strauss for helpful discussions. This work is supported by NSF grants AST93-15368, ASC93-18185 and NASA grant NAG5-2759. XF thanks the support from an Advisory Council Scholarship.

REFERENCES

- Bahcall, N.A., & Cen, R., 1992, ApJ, 398, L81
- Bahcall, N.A., & Cen, R., 1993, ApJ, 409, L48
- Bahcall, N.A., Lubin, L., & Dorman, V., 1995, ApJ, 447, L81
- Bahcall, N.A., Fan, X., & Cen, R., 1997, to be submitted to ApJ
- Bunn, E.F., & White, M., 1996, astro-ph/9607060
- Carlberg., R.G., Yee, H.K.C., Ellingson, E., Abraham, R., Gravel, P., Morris, S.M., & Pritchett, C.J., 1996, ApJ, 462, 32
- Carlberg., R.G., Morris, S.M., Yee, H.K.C., & Ellingson, E., 1997, ApJL, 479, L19
- Castander, F.J., Ellis, R.S., Frenk, C.S., Dressler, A., & Gunn, J.E., 1994, ApJ, 424, L79
- Cen, R., & Ostriker, J.P., 1994a, ApJ, 429, 4
- Cen, R., & Ostriker, J.P., 1994b, ApJ, 431, 451
- Collins, C.A., Burke, D.J., Romer, A.K., Sharples, R.M., & Nichol, R.C., 1997, ApJL, in press
- Eke, V.R., Cole, S., & Frenk, C.S., 1996, MNRAS, 282, 263
- Fan, X., Bahcall, N.A., & Cen, R., 1997, to be submitted to ApJ
- Henry, J.P., & Arnaud, K.A., 1991, ApJ, 310, 31
- Henry, J.P., Gioia, I.M., Maccacaro, T., Morris, S.L., Stocke, J.T., & Wolter, A., 1992, ApJ, 386, 408
- Hughes, J.P., 1989, ApJ, 337, 212
- Jing, Y.P., & Fang, L.-Z., 1994, ApJ, 432, 438
- Luppino, G.A., & Gioia, I.M., 1995, ApJ, 445, L77
- Mazure, A., et al., 1996, A&A, 310, 31
- Mushotzky, R.F., & Scharf, C.A., 1997, ApJL, in press

- Nichol, R.C., Holden, B.P., Romer, A.K., Ulmer, M.P., Burke, D.J., & Collins, C.A., 1997, ApJ, in press
- Ostriker, J.P., 1993, ARA&A, 31, 689
- Peebles, P.J.E., 1993, *Principles of Physical Cosmology* (Princeton University Press : Princeton)
- Peebles, P.J.E., Daly, R.A., & Juskiewicz, R., 1989, ApJ, 347, 563
- Pen, U.-L., 1997, ApJ, submitted
- Postman, M., Lubin, L., Gunn, J.E., Oke, J.G., Schneider, D.P., & Christensen, J.A., 1996, ApJ, 111, 615
- Press, W.H., & Schechter, P., 1974, ApJ, 187, 425
- Viana, P.P., & Liddle, A.R., 1996, MNRAS, 281, 323
- Walter, C., & Klypin, A., 1996, ApJ, 462, 13
- White, S.D.M., Efstathiou, G., & Frenk, C.S., 1993, MNRAS, 262, 1023

Table 1. Model Parameters

	Ω	Λ	h	σ_8
SCDM	1.0	0.0	0.5	1.05
SCDM	1.0	0.0	0.5	0.53
MDM	1.0	0.0	0.5	0.60
OCDM	0.35	0.0	0.7	0.80
LCDM	0.4	0.6	0.65	0.79

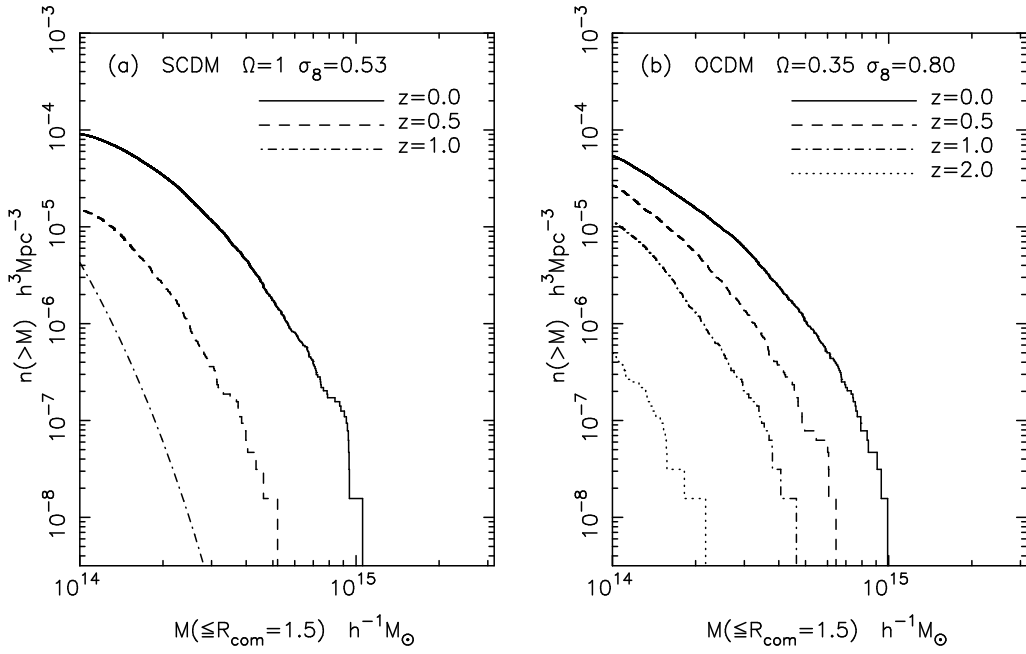


Figure 1. The evolution of the cluster mass function with redshift, for cluster masses within a co-moving radius $R_{\text{com}} = 1.5h^{-1}$ Mpc. (For $z=1$ in SCDM $\sigma_8 = 0.53$, Press-Schechter approximation is used.)

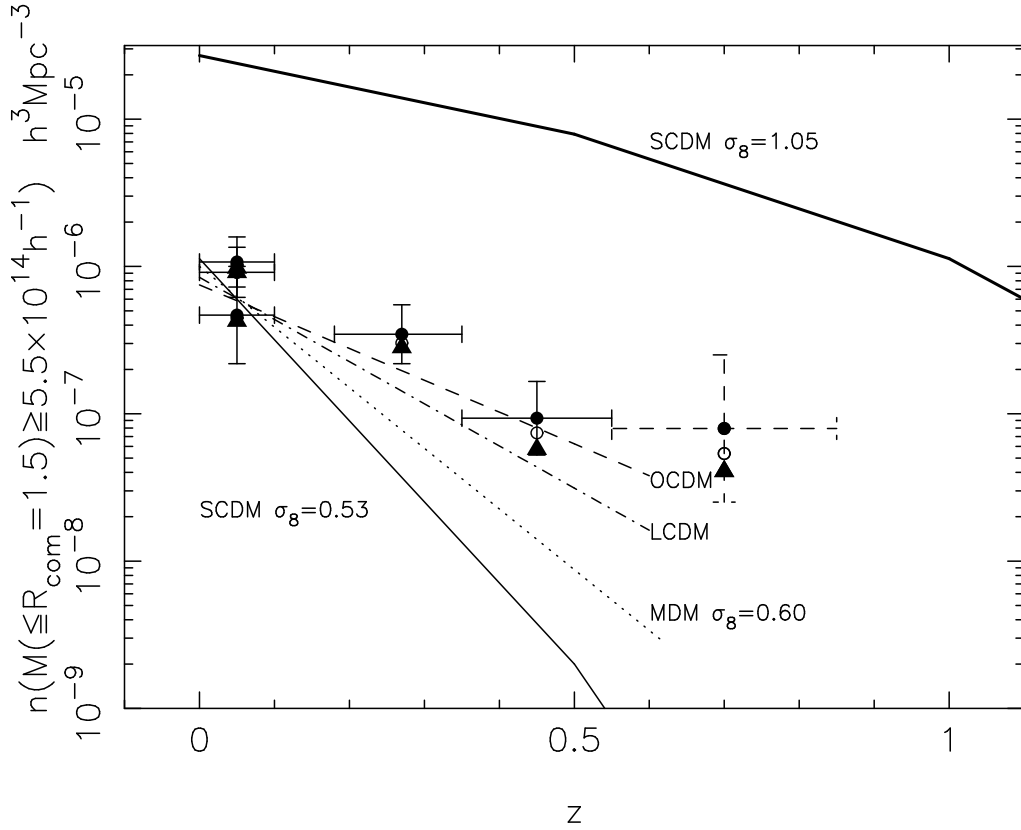


Figure 2. Observed vs. model cluster abundance as a function of redshift for clusters with mass $M(\leq R_{\text{com}} = 1.5h^{-1}\text{Mpc}) \geq 5.5 \times 10^{14}h^{-1}M_{\odot}$. The observed abundance at $z \sim 0$ are from Bahcall and Cen (1992), Mazure *et al.* (1996) and Henry and Arnaud (1992). The data at $z \sim 0.27$ and 0.45 are from the CNOC survey (Carlberg *et al.* 1997), and at $z \sim 0.7$ from Luppino and Gioia (1995). The different symbols represent the observed number densities for $\Omega=1$ (filled circles), $\Omega=0.35$, $\Lambda=0$ (open circles), and $\Omega=0.4$, $\Lambda=0.6$ (triangles).

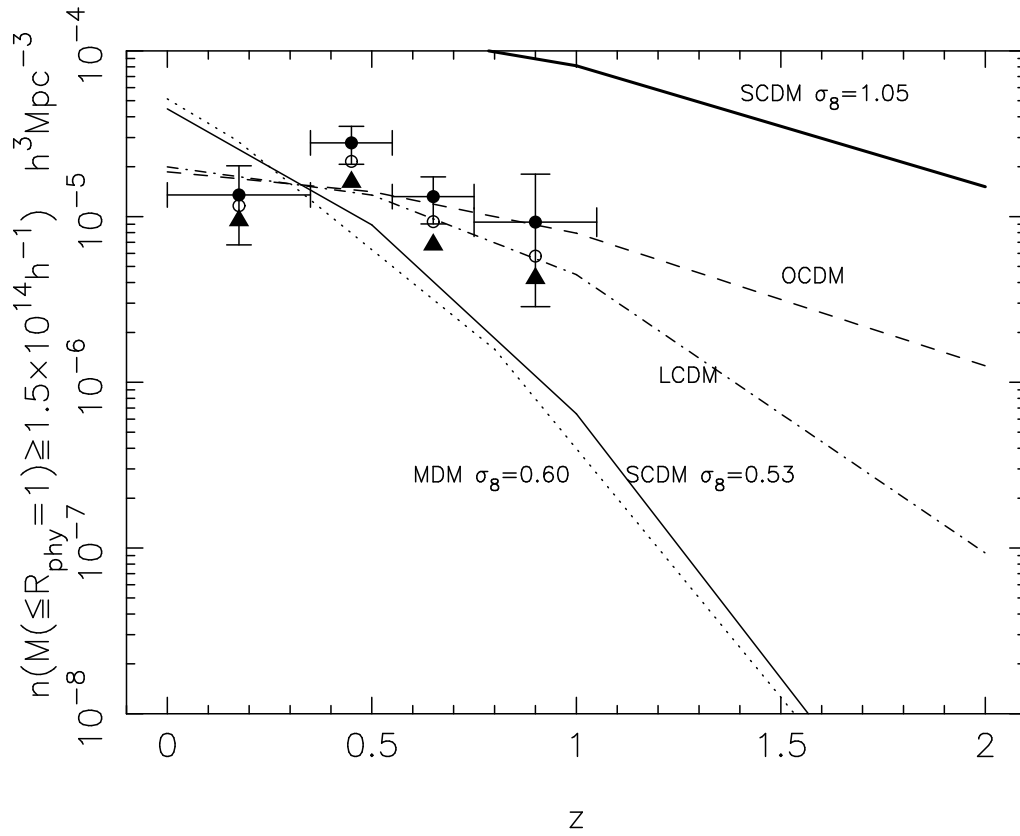


Figure 3. Observed vs. model cluster abundance as a function of redshift for clusters with mass $M(\leq R_{\text{phy}} = 1.0h^{-1}\text{Mpc}) \geq 1.5 \times 10^{14}h^{-1}M_{\odot}$. The data are from the PDCS survey (Postman *et al.*, 1996). The different symbols for the data are the same as in Fig. 3.

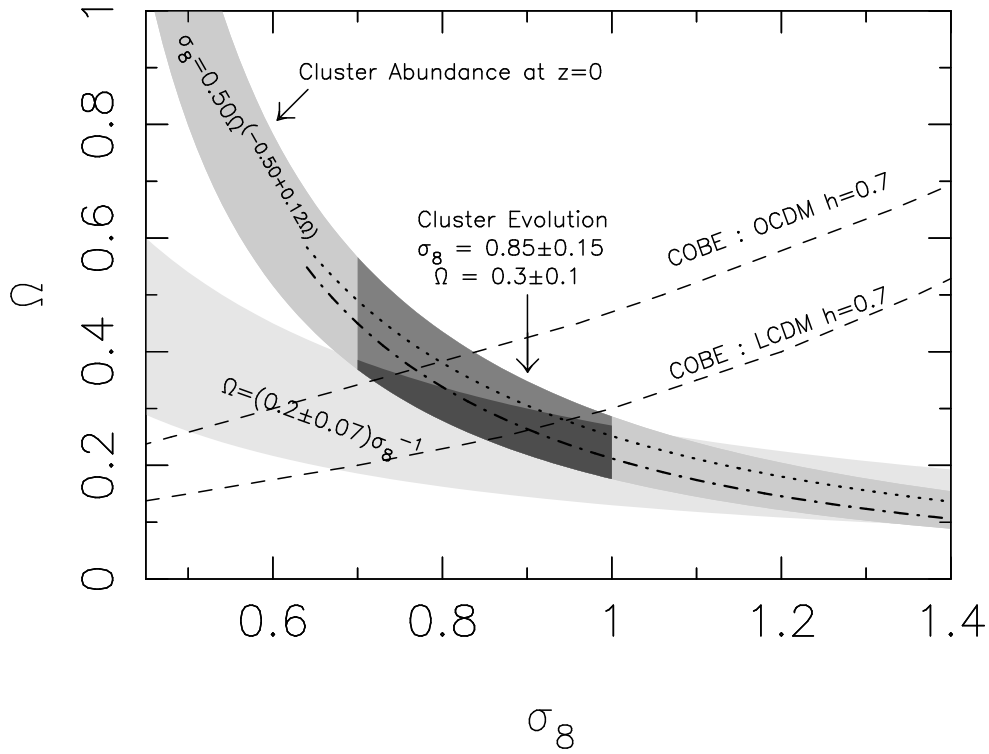


Figure 4. Observational constraints on Ω and σ_8 . The band $\sigma_8 = 0.50\Omega^{-0.50+0.12\Omega}$ represents the range due to the present day cluster abundance (for the average of open and Λ models, Eke *et al.* 1996; the inserted dash-dotted and dotted lines are the best fits for open and Λ models, respectively). The darker band of $\sigma_8 = 0.85 \pm 0.15$, $\Omega = 0.3 \pm 0.1$ is the constraint placed in this paper by cluster evolution (§5). The $\Omega = (0.2 \pm 0.07)\sigma_8^{-1}$ band represents cluster dynamics constraint. The dashed lines are the COBE four year data (Bunn and White 1996). A low-density low-bias universe with $\Omega = 0.3 \pm 0.1$ and $\sigma_8 = 0.85 \pm 0.15$ best fits all the data (darkest region), with cluster evolution providing the tightest constraint.